Tamoxifen-like metallocifens target the thioredoxin system determining mitochondrial impairment leading to apoptosis in Jurkat cells

Valeria Scalcon, Michèle Salmain, Alessandra Folda, Siden Top, Pascal Pigeon, Hui Zhi Shirley Lee, Gérard Jaouen, Alberto Bindoli, Anne Vessieres, Maria Pia Rigobello

Tamoxifen-like metallocifens target the thioredoxin system determining mitochondrial impairment leading to apoptosis in Jurkat cells

Valeria Scalcon,[a*] Michèle Salmain,[b*] Alessandra Folda,[a] Siden Top,[b] Pascal Pigeon,[bc] Hui Zhi Shirley Lee,[bc] Gérard Jaouen,[bc] Alberto Bindoli,[d] Anne Vessières[b**] and Maria Pia Rigobello [a**]

a) Dipartimento di Scienze Biomediche, Università di Padova, Via Ugo Bassi 58/b, 35131 Padova, Italy

b) Sorbonne Universités, UPMC Univ Paris 06, CNRS, Institut Parisien de Chimie Moléculaire (IPCM), F-75005 Paris, France

c) Chimie ParisTech, 11 rue Pierre et Marie Curie, F-75005 Paris, France

d) Istituto di Neuroscienze (CNR) Sezione di Padova, c/o Dipartimento di Scienze Biomediche, Via Ugo Bassi 58/b, 35131 Padova, Italy

* Valeria Scalcon and Michèle Salmain contributed equally to the work

** Anne Vessières and Maria Pia Rigobello: co-corresponding authors

Tamoxifen-like metallocifens (TLMs) of the group-8 metals (Fe, Ru, and Os) show strong anti-proliferative activity on cancer cell lines resistant to apoptosis, owing to their unique redox properties. In contrast, the thioredoxin system, which is involved in cellular redox balance, is often overexpressed in cancer cells, especially in tumour types resistant to standard chemotherapies. Therefore, we investigated the effect of these three TLMs on the thioredoxin system and evaluated the input of the metallocene unit in comparison with structurally related organic tamoxifens. *In vitro*, all three TLMs became strong inhibitors of the cytosolic (TrxR1) and mitochondrial (TrxR2) isoforms of thioredoxin reductase after enzymatic oxidation with HRP/H_2O_2 while none of the organic analogues was effective. In Jurkat cells, TLMs inhibited mainly TrxR2, resulting in the accumulation of oxidized thioredoxin 2 and cell redox imbalance. Overproduction of ROS resulted in a strong decrease in the mitochondrial membrane potential, translocation of cytochrome *c* to the cytosol and

activation of caspase 3, thus leading to apoptosis. None of these events occurred with organic tamoxifens. The mitochondrial fraction of cells exposed to TLMs contained a high amount of the corresponding metal, as quantified by ICP-OES. The lipophilic and cationic character associated with the singular redox properties of the TLMs could explain why they alter the mitochondrial function. These results provide new insights into the mechanism of action of tamoxifen-like metallocifens, underlying their prodrug behaviour and the pivotal role played by the metallocenic entity in their cytotoxic activity associated with the induction of apoptosis.

Significance to metallomics

The biological effects of tamoxifen-like metallocifens (TLMs) of iron, ruthenium and osmium on Jurkat cells were compared to those of the corresponding organic tamoxifens. All three TLMs behaved as strong inhibitors of mitochondrial thioredoxin reductase both *in vitro* and in Jurkat cells, and induced mitochondrial membrane depolarization and eventually cell apoptosis. The organic molecules were inactive in this set of experiments, thus underlying the role of the metals. These effects are associated with the unique redox properties of the metallocene units and charge-driven accumulation of TLMs in mitochondria. Among the three compounds, the ferrocenyl TLM appeared to be the most active.

Introduction

Breast cancer remains the most common malignancy in women, and despite the efforts that have been expended on its early detection, half a million people died from this disease in 2012.[1] Early breast cancer is now considered potentially curable and tamoxifen administration is the standard endocrine therapy of hormone receptor positive breast cancer. This is not the case for metastatic breast cancers, which are heterogeneous, often resistant to apoptosis and consequently difficult to cure. Thus, the search for new drugs with mechanisms of action different from those already in use is urgently needed. Some of us introduced some time ago the ferrocenyl analogues of **OH-tamoxifen** (**OH-Tam[2]**, Chart 1), an active metabolite of tamoxifen.[2,3] Not only did these compounds have an anti-oestrogenic effect on hormone-dependent breast cancer cells, but they also displayed high cytotoxicity on the triple negative breast cell line MDA-MB-231 (IC_{50} = 0.5 µM for **Fc-OH-Tam**)[3] as well as on a panel of cells resistant to apoptosis (glioma and melanoma).[4,5]

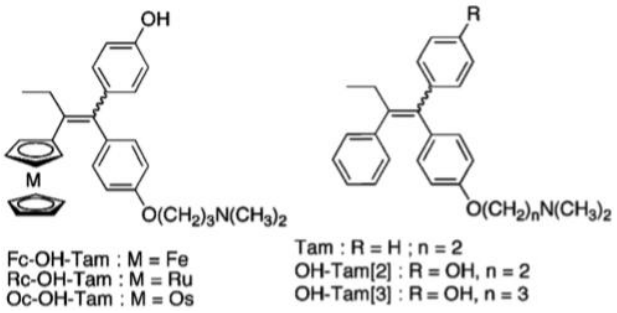

Chart 1 Formulae of the compounds under study.

In addition, **Fc-OH-Tam** significantly inhibited *in vivo* growth of MDA-MB-231 xenografted tumours in mice when formulated in lipid nanocapsules (LNCs).[4] Regarding the mechanism of action of this complex, we found that **Fc-OH-Tam** induced strong senescence in MDA-MB-231 and low apoptosis.[6] These remarkable properties have been linked to the presence of the [Fc-ene-phenol] motif that is selectively activated in cancer cells, therefore revealing their redox environment.[7] As such, **Fc-OH-Tam** acts as a prodrug whose cytotoxicity is associated with its oxidation to a highly electrophilic quinone methide.[7] More recently we found that the quinone methide of **Fc-OH-Tam** was able to strongly inhibit the enzyme thioredoxin reductase (TrxR) *in vitro*.[8] TrxR belongs to the thioredoxin system, which, together with the glutathione system, is responsible for thiol redox homeostasis. It is present as cytosolic (TrxR1) and mitochondrial (TrxR2) isoforms, displaying a selenocysteine residue at its C-terminal active site, which acts as a major target of electrophiles as well as many metal complexes.[9-12] TrxR is often overexpressed in cancer cells and its inhibition may lead to cell apoptosis.[13,14] **Fc-OH-Tam** inhibits TrxR in Jurkat cells, indicating that its conversion to quinone methide occurs *in cellulo via* endogenous oxidizing systems. Recent studies on the tamoxifen-like complex of osmium (**Oc-OH-Tam**, Chart 1) showed that *in vitro* inhibition of TrxR only occurred after its enzymatic oxidation by the HRP/H_2O_2 mixture. Although less cytotoxic than **Fc-OH-Tam** on the MDA-MB-231 cell line (IC_{50} = 2.7 µM),[15] **Oc-OH-Tam** proved to be an effective inhibitor of TrxR in Jurkat cells, inducing mitochondrial dysfunction and cell death.[16]

To gain better insight into the mechanism of action of tamoxifen-like metallocifens (TLMs) and to evaluate the role played by the metallocenic unit we report here the comparison of some biological effects of TLMs of iron, ruthenium and osmium with those of their organic tamoxifen analogues (Chart 1). Experiments included *in vitro* studies on purified cytosolic and mitochondrial isoforms of TrxR (TrxR1 and TrxR2) followed by studies on

mitochondrial functionality in Jurkat cells. In particular, the redox state of mitochondrial Trx, ROS level and mitochondrial membrane potential (MMP) were measured. In addition, the intracellular distribution of metals was determined using ICP-OES measurements. Overall, only TLMs and not their organic analogues were able to initiate cell apoptosis *via* a mitochondria-mediated pathway.

Experimental

Materials

Stock solutions of the compounds (1×10^{-2} M) were prepared in DMSO and were stable for at least two months if kept at 4 °C. Horseradish peroxidase (HRP), yeast glutathione reductase, **Tam**, **OH-Tam[2]**, iodoacetamide (IAM), iodoacetic acid (IAA), DTNB and metal standards were purchased from Sigma Aldrich (Saint Louis, MO, USA). BIAM, TMRM, DHR and MitoSOX were purchased from Invitrogen (Thermo Fisher Scientific, Waltham, MA, USA). Primary antibodies were utilized: Trx2 monoclonal antibody (H75) and caspase-3 polyclonal antibody clone H-277 (Santa Cruz Biotechnology, Santa Cruz, CA, USA); cytochrome *c* clone 7H8.C12 (BioSource International, Inc., Camarillo, CA, USA); anti-cytochrome *c* oxidase subunit 4 monoclonal antibody 1D6 (Thermo Fisher Scientific, Waltham, MA, USA).

Enzymatic oxidation of the compounds by the HRP/H_2O_2 mixture

Enzymatic oxidation of the compounds (25–50 µM) by HRP (46 nM) and H_2O_2 (200 µM) was performed at pH 8.1 in buffer (0.2 M Tris–HCl, 1 mM EDTA) containing 10% DMSO. HRP (40 µL of 1.14 µM solution) and H_2O_2 (20 µL of 10 mM solution) were pre-incubated for 5 min and then added to the solution of the compounds (940 µL). The solution was immediately transferred to a cuvette and the UV-Visible spectrum was recorded between 250 and 600 nm every 30 s on a Cary 50 spectrometer (Varian, Palo Alto, CA, USA). Rate constants k_{obs} were calculated using Kaleidagraph software by fitting OD_{324nm} (**Oc-OH-Tam**), OD_{413nm} (**Fc-OH-Tam**), OD_{418nm} (**Rc-OH-Tam**) and OD_{279nm} (**OH-Tam[3]**) *versus* time data according to the first order law equation: $OD = C_0 + C_1 \times \exp(-k_{obs} \times t)$.

Enzymatic activity estimation of isolated TrxR1 and TrxR2

Highly purified cytosolic (TrxR1) and mitochondrial (TrxR2) thioredoxin reductases were prepared from rat liver according to Luthman and Holmgren[17] and Rigobello and Bindoli,[18] respectively. The protein content of the purified enzyme preparations was measured according to Lowry *et al.*[19] Thioredoxin reductase activity was determined by estimating the DTNB- reducing properties of the enzymes in the presence of NADPH. Aliquots of highly purified TrxR1 or TrxR2 in 0.2 M Tris–HCl buffer (pH 8.1), 1 mM EDTA and 0.25 mM NADPH were pre-incubated for 5 min with various compounds. Afterwards, the reaction was initiated with 1 mM DTNB and monitored spectrophotometrically at 412 nm for about 10 min. For the formation of oxidized metallocifen derivatives, freshly prepared compounds at increasing concentrations were incubated for 15 min in 0.2 M Tris–HCl buffer (pH 8.1) containing 1 mM EDTA, 0.1 mM H_2O_2 and 22 nM HRP. Then, TrxR aliquots and 0.25 mM NADPH were added and incubated for 5 min. Finally, the reaction was initiated with 1 mM DTNB and monitored spectrophotometrically at 412 nm for about 10 min.

BIAM assay

First, TLMs and organic tamoxifen were treated with the mixture of 22 nM HRP/0.1 mM H_2O_2 for 15 min as reported in the previous paragraph. Then, 1 µM TrxR pre-reduced in the presence of 60 µM NADPH was incubated with 2 µM of the obtained derivatives for 30 min at room temperature, in 50 mM Tris–HCl buffer (pH 7.4) containing 200 µM NADPH and 1 mM EDTA. After incubation, 8 µL of the reaction mixture was added to 8 µL of 100 µM biotinylated iodoacetamide (BIAM) in 0.1 M Tris–HCl at pH 8.5 or in 0.1 M Hepes-Tris pH 6.0.[20] The samples were incubated at room temperature for an additional 30 min to allow BIAM alkylation of free –SH/SeH groups of the enzyme. Then, BIAM-modified enzyme was subjected to sodium dodecyl sulphate-polyacrylamide gel electrophoresis (SDS-PAGE) on a 10% gel, and transferred to a nitrocellulose membrane. BIAM labelled enzyme was detected with horseradish peroxidase-conjugated streptavidin and enhanced chemiluminescence detection.

Determination of total thioredoxin reductase activity in Jurkat cell lysates

The human leukemic lymphoblastoid Jurkat cells were cultured in RPMI 1640 medium

supplemented with 2 mM L-glutamine, 10% FBS and 1% penicillin/streptomycin (Invitrogen) at 37 °C in a humidified atmosphere of 95% air and 5% CO_2. Cells (2×10^6) were incubated with 15 μM compounds for 18 h, then harvested and washed with PBS. Each sample was lysed with a modified RIPA buffer: 150 mM NaCl, 50 mM Tris–HCl, 1 mM EDTA, 1% Triton X-100, 0.1% SDS, 0.5% DOC, 1 mM NaF and an antiprotease cocktail (‘‘Complete’’ Roche, Mannheim, Germany) containing 0.1 mM PMSF. After 40 min at 4 °C, the lysates were centrifuged at 12 000*g* for 6 min. The supernatants were tested for total TrxR activity. Therefore, aliquots of lysates (12 μg proteins) were incubated for 40 min in a final volume of 50 μL in 100 mM Hepes–Tris buffer (pH 7.6) in the presence of 15 mM EDTA, 1.5 mM NADPH, 0.20 mM insulin, and 100 μM Trx from *E. coli*. The reaction was stopped by adding 0.2 mL of 1 mM DTNB in 0.2 M Tris–HCl buffer (pH 8.1) containing 1 mM EDTA and 7.2 M guanidine, and the samples' O.D. was estimated at 412 nm[21] on a plate reader (Tecan Infinite® M200 PRO, Männedorf, CH).

Preparation of cytosol and mitochondria enriched fractions and evaluation of thioredoxin reductase activity

To obtain cytosolic and mitochondrial fractions, Jurkat cells (3×10^7) were grown in 75 cm^2 flasks and then treated with various compounds (30 μM) for 18 h. After incubation, the cells were processed to obtain mitochondria and cytosol enriched fractions essentially following the protocol of Clayton and Shadel.[22] Briefly, the cells were collected, washed with PBS and subjected to hypo-osmotic treatment with 2 mL of 10 mM NaCl, 1.5 mM $MgCl_2$ and 10 mM Tris–HCl (pH 7.5) for 5 min and gently homogenized using a Dounce tissue grinder. After this treatment, 1.4 mL of 525 mM mannitol, 175 mM sucrose, 12.5 mM Tris–HCl (pH 7.5) and 2.5 mM EDTA (pH 7.5) were rapidly added. Then, the homogenate was diluted to a final volume of 5 mL with 210 mM mannitol, 70 mM sucrose, 5 mM Tris–HCl (pH 7.5) buffer, and 1 mM EDTA (pH 7.5) and subjected to differential centrifugation. The first step was carried out at 1300*g* for 5 min at 4 °C to discard nuclei and non-disrupted cells. The mitochondrial fraction was pulled down from the supernatant at 15 800*g* for 15 min at 4 °C and washed twice. The crude soluble supernatant obtained from the mitochondrial isolation step was further centrifuged at 105 000*g* for 15 min to obtain the cytosolic fraction. Afterwards, mitochondrial samples were lysed using a modified RIPA buffer, as reported in the previous paragraph, and subjected to protein

determination with the Lowry assay.[19] In addition, the presence of cytochrome oxidase as a mitochondrial marker was assessed by Western blot analysis using an anti-cytochrome *c* oxidase subunit 4 monoclonal antibody 1D6. Both cytosolic and mitochondrial fractions (50 µg of proteins) were then tested for thioredoxin reductase activity in a buffer containing 0.2 M NaKPi, 5 mM EDTA (pH 7.4) and 20 mM DTNB. After 2 min, 0.25 mM NADPH was added and the reaction was followed at 412 nm at 25 °C using a Lambda 2 spectrophotometer (PerkinElmer, Waltham, MA, USA).

Redox Western blot analysis of Trx2

The redox state of Trx was detected using a modified Western blot analysis.[23,24] Briefly, after treatment with the compounds (15 µM) for 18 h, Jurkat cells (2 x 10^6) were washed with PBS and lysed in 100 µL of urea lysis buffer (100 mM Tris–HCl, pH 8.3, containing 1 mM EDTA, 8 M urea, and 10 mM IAM) in order to alkylate free thiols. Incubation was carried out at 37 °C for 20 min. Then, the cell lysates were spun down and precipitated by ice-cold acetone-1 M HCl (98 : 2). The pellets were washed twice with ice-cold acetone–1 M HCl–H_2O (98 : 2 : 10), re-suspended in 60 µL of urea lysis buffer including 3.5 mM DTT, and incubated for 30 min at 37 °C to reduce the disulfide bonds. Afterwards, 3 µL of 600 mM IAM (final concentration 30 mM) were added to the samples, followed by incubation for 30 min at 37 °C. The protein concentration was determined using the Lowry assay.[19] The proteins were separated by urea-PAGE (7% acrylamide/bis(acrylamide) in 7 M urea) and blotted on a nitrocellulose membrane using a Trans-Blot® Turbot™ System (Bio-Rad Laboratories, Hercules, CA, USA). The membranes were probed with the primary antibody for Trx2 (H75).

Flow cytometric analysis of the mitochondrial membrane potential and superoxide production in Jurkat cells

The drug-influenced cell mitochondrial membrane potential was analyzed by flow cytometry with the fluorescent probe tetramethyl rhodamine methyl ester (TMRM). Jurkat cells (2 x 10^6) were treated for 18 h with the compounds (15 µM) and then harvested and re-suspended in PBS/10 mM glucose/25 nM TMRM (final concentration) for 15 min at 37 °C

in the dark. Induced changes of the membrane potential were estimated with a FACSCanto™ II flow cytometer (Becton-Dickinson, CA, USA) using an argon laser at 585 nm. Cells cultured and treated under the same conditions described above were also probed for mitochondrial superoxide production utilizing the fluorescent probe MitoSOX™ Red. After treatment with the complexes, Jurkat cells (5×10^5) were incubated with 1 µM MitoSOX™ in PBS/10 mM glucose for 25 min in the dark, then diluted (1 : 4) and analyzed on a FACSCanto™ using an argon laser at 585 nm.

Determination of short-term cellular ROS production in Jurkat cells

Jurkat cells (4×10^5 per well) were seeded in a 96 well plate in PBS/10 mM glucose and then incubated for 1 h with 15 µM dihydrorhodamine 123 (DHR) at 37 °C, 5% CO_2. Afterwards, the medium was removed and to each well 100 µM PBS/10 mM glucose supplemented with 10 µM TLMs or organic tamoxifen derivatives was added. Finally, ROS production was estimated by monitoring the fluorescence increase of the probe (λ_{Ex} = 500 nm, λ_{Em} = 536 nm), using a Tecan Infinite® M200 PRO plate reader.

Estimation of cytochrome *c* release and caspase-3 activation

Cytochrome *c* release and caspase-3 activation were detected using the Western blot technique. After 18 h of incubation in the presence of 15 µM of the compounds, Jurkat cells (2×10^6) were harvested, washed with PBS, and treated with a hypotonic lysis buffer (20 mM Hepes-Tris buffer (pH 7.5), 10 mM KCl, 1.5 mM $MgCl_2$, 1 mM EDTA and 1 mM EGTA) added with an antiprotease cocktail (Complete, Roche, Mannheim, DE) for 15 min. Then, the suspension was centrifuged at 12 500*g* for 10 min at 4 °C. The supernatant added with 0.5 mM EGTA and 2.5 mM PMSF was centrifuged for 30 min at 100 000*g* at 4 °C to obtain the cytosolic fraction. The pellet obtained from the first centrifugation was lysed in the previously reported modified RIPA buffer. Aliquots of 10 µg protein of the supernatants or of the pellets were subjected to SDS-PAGE (15%) followed by Western blot using a cytochrome *c* monoclonal antibody clone 7H8.C12 and a caspase-3 polyclonal antibody clone H-277. A peroxidase-conjugated secondary antibody and

chemiluminescence were used to detect the immunoreactive bands.

Metal quantification in Jurkat cell compartments by ICP-OES

Jurkat cells (3×10^7 cells) incubated for 24 h in the presence of the compounds (30 µM) were subjected to cell fractionation, as reported in a previous paragraph. For the ICP-OES experiments, mitochondria and crude nuclei fractions were dissolved in 0.54 mL HCl (37%, Fluka for trace analysis) and digested at 60 °C in an ultrasound bath for 1 h. Then, the samples' volume was brought to 10 mL by the addition of water ([HCl] in the sample = 2%). The cytosol samples were adjusted to 2% HCl by the addition of appropriate volumes of 37% HCl and water (final volume = 10 mL). All the solutions were filtered on a 0.45 µm syringe filter. Quantification of iron, ruthenium and osmium was performed at 238.204, 267.876 and 225.585 nm, respectively, using an Agilent 5100 instrument (Santa Clara, CA, USA). Metal standards (Fe, Ru and Os) were prepared from 1000 ppm stock solutions. The concentrations used for calibration were in all cases 0, 7.8, 15.6, 31.2, 62.5, 125, 250 and 500 ppb. Measurements were done in triplicate in two or three sets of independent experiments. HCl was used instead of HNO_3 as the latter leads to the formation of the highly toxic and volatile OsO_4. The ICP-OES experiments were performed on the ALIPP6 platform at the University Pierre et Marie Curie.

Statistical analysis

All the experimental data reported, if not indicated, are the mean with their respective SD of at least 4 experiments. The statistical analyses of variance (ANOVA) were performed using the Tukey test with INSTAT 3.3 (GraphPad) software.

Results

Synthesis

The TLMs of the group-8 metals **Fc-OH-Tam**, **Rc-OH-Tam** and **Oc-OH-Tam** (Chart 1)

used in this study were prepared by following the previously reported protocols and are stable for months in the solid state.[3,15,25] The TLMs were obtained as a mixture of *Z* and *E* stereomers. We previously found that these stereomers rapidly isomerize in protic medium. Thus, the experiments reported herein were performed with mixtures of (*Z* + *E*) isomers of the 3 complexes. The biochemical behaviour of the TLMs was systematically compared to that of 3 analogous organic tamoxifens, namely Tam, its active metabolite **OH-Tam[2]**, and **OH-Tam[3]**, the organic analogue including the same dimethylamino-terminated side chain as in the three TLMs, which was prepared according to the literature.[26]

Identification of the products of enzymatic oxidation by the HRP/H_2O_2 mixture

Enzymatic oxidation of the TLMs and their organic counterparts by the HRP/H_2O_2 mixture was monitored by UV-visible spectrometry. For **Fc-OH-Tam**, the progressive appearance of an intense band at 402 nm was observed, which was readily assigned to quinone methide by comparison with the authentic product obtained by chemical oxidation with Ag_2O (Fig. S1-A, ESI†).[7,27] This conversion corresponds to a 2-electron, 2-proton abstraction pathway. The same behaviour was found for **Rc-OH-Tam** for which a band at 418 nm was observed upon oxidation with HRP/H_2O_2 (Fig. S1-B, ESI†). In contrast, enzymatic oxidation of **OH-Tam[3]** led to the rapid disappearance of its characteristic band at 279 nm but no new peak appeared on the spectra (Fig. S1-C, ESI†). Thus, treatment of **OH-Tam[3]** by HRP/H_2O_2 did not afford quinone methide, which is characterized by an intense band at around 400 nm.[28] Previous literature data demonstrate that HRP oxidation of **OH-Tam[2]** rather affords unstable radical species that tend to polymerize.[29] We previously found that enzymatic oxidation of **Oc-OH-Tam** did not afford quinone methide as did chemical oxidation with Ag_2O but rather led to a quinone methide carbocation characterized by a band at 331 nm resulting from a two-electron, 1-proton abstraction pathway.[16] This unusual behaviour was assumed to originate from the high stability of carbenium ions derived from osmocene derivatives.[30,31] Table 1 summarizes the oxidation pathway of the compounds under study and the rate constants of oxidation upon treatment with HRP/H_2O_2. As it appears, oxidation of all the compounds proceeded swiftly, with a slightly faster rate observed for ferrocifen than for ruthenocifen and osmocifen.

Table 1 Summary of the enzymatic oxidation experiments

Compound	Oxidation pathway	λ_{max} (nm)	Nature of oxidation product	Rate constant of oxidation (min^{-1})
Fc-OH-Tam	$-2e^-/-2H$[a]	402	QM	0.521 ± 0.022[d]
Rc-OH-Tam	$-2e^-/-2H$	418	QM	0.319 ± 0.008[d]
Oc-OH-Tam	$-2e^-/-1H$[b]	331	QM	0.305 ± 0.002[d]
OH-Tam[3]	$-1e^-/-1H$[c]	None	n.d.	0.471 ± 0.02[e]

[a] Data from ref. 8. [b] Data from ref. 16. [c] Data from ref. 29. [d] Rate constant of QM or QM^+ formation. [e] Rate constant of substrate disappearance.

In vitro inhibition studies on TrxR1 and TrxR2

The possible inhibitory activity of the three TLMs and the three organic analogues was first investigated on TrxR1 and TrxR2 purified from the rat liver. Experimentally, mixtures of pre-reduced TrxR1 or TrxR2 and various concentrations of each compound were incubated for 5 min before their enzymatic activity was measured. Table 2 lists the IC_{50} values deduced from these experiments.

Both **Fc-OH-Tam** and **Oc-OH-Tam** were moderate inhibitors of both TrxR1 and TrxR2, with IC_{50} values between 15 and 23 µM, while **Rc-OH-Tam** was slightly active on TrxR1 and inactive on TrxR2. In contrast, none of the organic counterparts was active on both TrxR1 and TrxR2. Strikingly different results were obtained when the TLMs were enzymatically oxidized by a mixture of HRP and H_2O_2 for 15 min prior to incubation with TrxR. Indeed, all three TLMs became potent inhibitors of TrxR1 with a remarkably low IC_{50} value of 60 nM for the iron complex, followed by an IC_{50} value of 0.42 µM for the ruthenium complex and 1.2 µM for the osmium complex. It is also interesting to note that oxidized **Fc-OH-Tam** was significantly more active on TrxR1 than on TrxR2. Conversely, preliminary treatment of **OH-Tam[2]** and **OH-Tam[3]** by HRP/H_2O_2 led to moderate inhibition of only TrxR1 (IC_{50} of *ca.* 8 µM) while HRP-treated Tam remained inactive on both TrxRs.

Table 2 *In vitro* inhibitory effect of tamoxifen-like metallocifens and organic tamoxifen derivatives on cytosolic (TrxR1) and mitochondrial (TrxR2) thioredoxin reductases

	IC_{50}[a] (μM)		IC_{50}[b] (μM) after treatment with H_2O_2/HRP	
Compound	TrxR1	TrxR2	TrxR1	TrxR2
Fc-OH-Tam	15 ± 2[c]	32 ± 3	0.06 ± 0.02	10.9 ± 1.2
Rc-OH-Tam	62 ± 2	4100	0.42 ± 0.08	4.6 ± 0.1
Oc-OH-Tam	40 ± 3.5	23 ± 3	1.2 ± 0.1[d]	3.9 ± 0.1
Tam	>100	>100	>10	>10
OH-Tam[2]	>100	>100	8.7 ± 1.1	>10
OH-Tam[3]	>100	>100	8.1 ± 0.8	>10

[a] Compounds were incubated with TrxR1 or TrxR2 in the presence of NADPH. After 5 min, TrxR activity was estimated as described in the Experimental section. [b] Compounds were incubated in 0.2 M Tris–HCl buffer (pH 8.1) containing 1 mM EDTA, with 22 nM HRP and 0.1 mM H_2O_2 for 15 min at 25 °C. The mixture was then incubated with TrxR1 or TrxR2 as indicated in footnote a. [c] Value from ref. 8. [d] Value from ref. 16.

Metallocifen interaction with the selenocysteine residue of TrxR

The C-terminal redox active site of TrxR is formed by a Cys–Sec motif (Sec = selenocysteine), which is the target of many electrophiles that inhibit TrxR by alkylation of Cys and/or Sec residues.

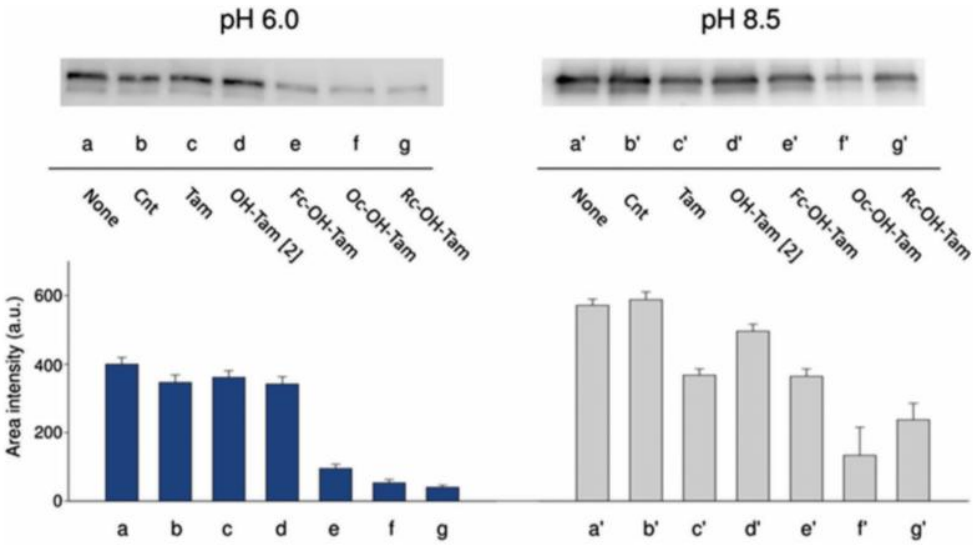

Fig. 1 BIAM assay of TrxR1 treated with compounds oxidized by HRP/H_2O_2. TLMs and Tam derivatives (2 μM) were treated with HRP/H_2O_2 for 15 min. The oxidized derivatives obtained (Ox-Mc with Mc = **Fc**, **Oc**, **Rc**; **Ox-OH-Tam[2]**, **Ox-Tam**) were incubated in the presence of a pre-reduced aliquot of TrxR1, as reported in the Experimental section. Then, aliquots of the reaction mixture were added to 50 μM biotinylated iodoacetamide (BIAM) in buffer at either pH 6.0 (0.1 M Hepes-Tris) or pH 8.5 (0.1 M Tris–HCl) to alkylate the –SH/–SeH remaining groups. Proteins were transferred to a nitrocellulose membrane, and BIAM conjugated enzyme was detected with a streptavidin–horseradish peroxidase conjugate. a, a' : **None**; b, b' : **Cnt**; c, c' : **Ox-Tam**; d, d' : **Ox-OH-Tam[2]**; e, e' : **Ox-Fc**; f, f' : **Ox-Oc**; g, g' : **Ox-Rc**.

Discrimination between both residues can be achieved by carrying out the biotin-iodoacetamide (BIAM) assay. As the pK_a values of both residues are different (pK_a R-SeH/R-Se^- = 5.24; pK_a R-SH/R-S^- = 8), selective alkylation by BIAM can be achieved according to the pH. At low pH (6), only the selenolate group of Sec is alkylated by BIAM, while at high pH (8.5) both the thiolate and the selenolate groups of Cys and Sec are simultaneously alkylated by BIAM.[32] Mixtures of TrxR1 and oxidized TLMs or organic tamoxifens were allowed to react with BIAM at pH 6 or 8.5 to alkylate the remaining selenolate and/or thiolate groups and the samples were subjected to the Western blot analysis (Fig. 1). Very weak bands were observed for TrxR1 samples exposed to the oxidized TLMs and then to BIAM at pH 6 while the organic analogues had no effect. As a consequence, the three oxidized TLMs equally interacted with Sec by probable alkylation of the highly nucleophilic selenolate group. When alkylation by BIAM was carried out at pH 8.5, the TrxR1 sample exposed to **Oc-OH-Tam** gave a band weaker than the control, indicating that only oxidized **Oc-OH-Tam** was able to simultaneously alkylate the thiol groups. In addition, the HRP/H_2O_2 mixture alone had no effect on the ability of BIAM to alkylate TrxR1 (cnt, lane b and b').

Activities of cytosolic and mitochondrial thioredoxin reductases in Jurkat cells

Jurkat cells (2×10^6) were incubated with each compound (15 µM) for 18 h. Then, the activity of total TrxR was determined in cell lysates (Fig. S2, ESI†). A large decrease of the total TrxR activity (60 to 95% inhibition) was observed in cells treated with the three TLMs while Tam and **OH-Tam[2]** induced a slight increase of activity and **OH-Tam[3]** had no effect. Additional experiments with **Fc-OH-Tam** showed that the activity of total TrxR was time-dependent as a slight increase was observed after 3 h followed by progressive and slow inhibition in the next 15 h (Fig. S3, ESI†). After optimization of the ratio between compounds (30 µM) and cell number (3×10^7), the activity of TrxR1 and TrxR2 was measured separately in the cytosolic and mitochondrial fractions of Jurkat cells (Fig. 2). High inhibition of TrxR2 was found for cells exposed to **Fc-OH-Tam** and **Rc-OH-Tam** (72% and 79.4% inhibition, respectively), while **Oc-OH-Tam** was less effective (44% inhibition). However, organic tamoxifens were significantly less potent (up to 27% inhibition). In contrast, the effect of the three TLMs on TrxR1 was less pronounced (25–36% inhibition)

and not much different from that of the organic compounds (12–21% inhibition).

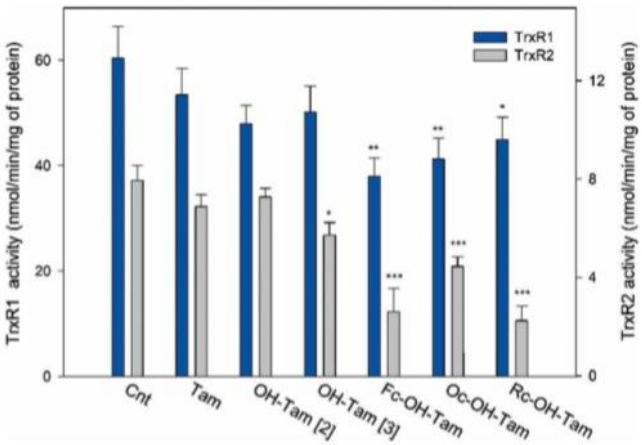

Fig. 2 TrxR1 and TrxR2 activities in Jurkat cells. Cytosolic and mitochondrial fractions were isolated from Jurkat cells treated with different compounds (30 µM/3 x 10^7 cells for 18 h), and TrxR activities were estimated as reported in the Experimental section. *: < 0.05; **: < 0.01; ***: < 0.001.

Mitochondrial thioredoxin (Trx2) redox state in Jurkat cells

As all three TLMs and not the organic analogues induced strong inhibition of TrxR2 in Jurkat cells, the redox state of Trx2 in cells exposed to each compound at 15 µM for 18 h was evaluated by the protein electrophoretic mobility shift assay with iodoacetamide/iodoacetic acid (IAM/IAA) as follows.[33] Lysates of cells incubated with each compound were first treated with IAM to titrate free SH groups, then, after reaction with DTT to reduce disulphide bonds, IAA was added in order to derivatize the SH groups arising from previously oxidized cysteines. The samples were submitted to urea-PAGE under non-reducing conditions and the 3 states of Trx2 (fully oxidized, partially oxidized and fully reduced) were detected by Western blot analysis (Fig. 3).

Cells incubated with the 3 TLMs showed the accumulation of the fully oxidized form of Trx2, especially those exposed to **Fc-OH-Tam** (90%) and to a lesser extent those exposed to **Rc-OH-Tam** and **Oc-OH-Tam** (57%). Conversely, the fully reduced form of Trx2 was predominant in cells exposed to Tam and **OH-Tam[2]** (77%). Only **OH-Tam[3]** induced the accumulation of a significant amount of oxidized forms of Trx2 (*ca.* 50%).

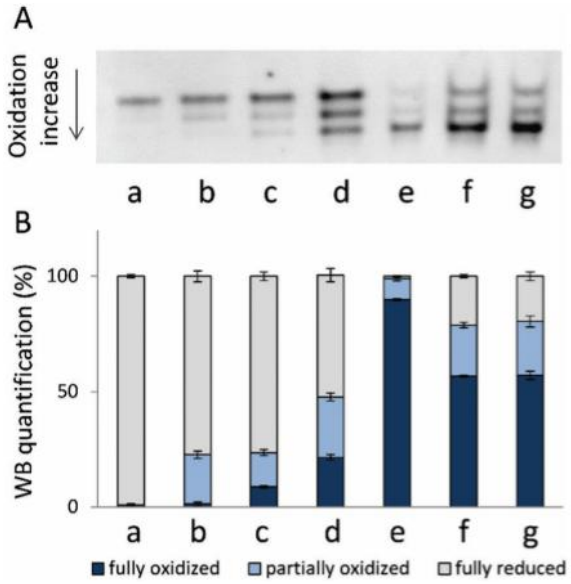

Fig. 3 Redox state of mitochondrial thioredoxin (Trx2) in Jurkat cells. Jurkat cells incubated for 18 h with 15 µM TLMs or organic tamoxifens were lysed and the lysates were treated with a 10 mM IAM/IAA procedure to titrate reduced, partially oxidized and fully oxidized thiol groups. The redox state of Trx2 was then detected by Western blot analysis (A). (a) **Cnt**; (b) **Tam**; (c) **OH-Tam[2]**; (d) **OH-Tam[3]**; (e) **Fc-OH-Tam**; (f) **Oc-OH-Tam**; (g) **Rc-OH-Tam**. (B) Densitometric analysis of the lanes was performed using ImageJ software.

ROS production and evaluation of the mitochondrial membrane potential (MMP) in Jurkat cells

Short-term (0–30 min) mitochondrial ROS production in Jurkat cells was first measured using the DHR dye, after cell incubation with 10 µM of the TLMs or organic tamoxifens. We found that the TLMs, but not the organic compounds, increased the basal ROS production during this period (Fig. S4, ESI†). The long-term mitochondrial superoxide level was then evaluated in Jurkat cells incubated with 15 µM TLMs or organic tamoxifens after 18 h, by flow cytometry analysis using MitoSOX™ Red as a fluorescent probe (Fig. 4 left). A very high percentage of cells (72%) incubated with **Fc-OH-Tam** emitted high MitoSOX™ fluorescence. This percentage was lower for cells incubated with **Rc-OH-Tam** and **Oc-OH-Tam** (around 40%) while the percentage of cells emitting high MitoSOX™ fluorescence was insignificant for those incubated with the organic tamoxifens (6–8%). The mitochondrial membrane potential (MMP) was evaluated on the same pool of cells by flow cytometry using the fluorescent dye TMRM (Fig. 4 right). The population of cells with a low MMP was close to 100% for cells incubated with the three TLMs for 18 h while the three organic tamoxifens affected the MMP to a much lower extent (up to 37.5% for **OH-**

Tam[3]). Interestingly, the rate of depolarization of the mitochondrial membrane was fast for **Fc-OH-Tam** since the percentage of cells displaying a low MMP was already equal to 42% after 3 h (Fig. S5, ESI†).

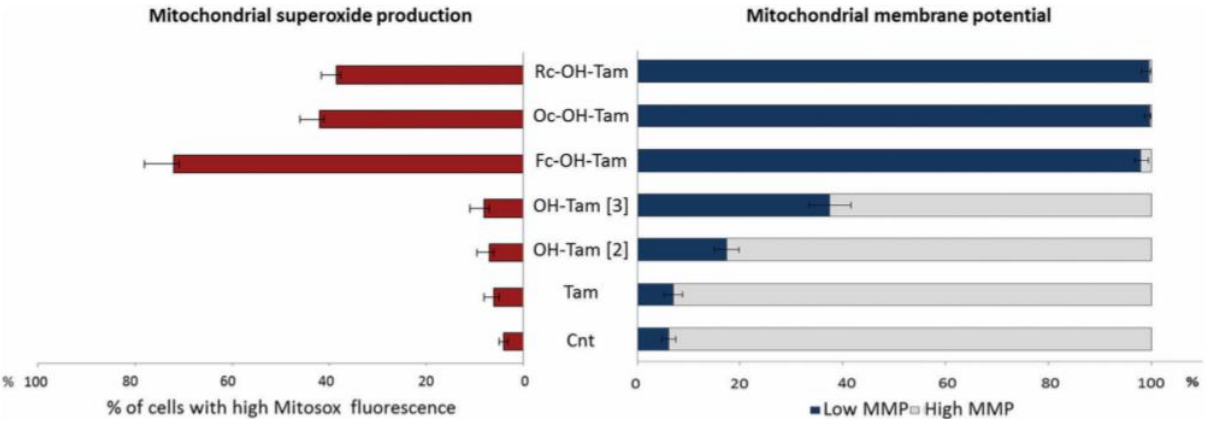

Fig. 4 Effects of TLMs and organic tamoxifens on mitochondrial superoxide production (left) and membrane potential (right) in Jurkat cells. Cells were treated for 18 h with various compounds (15 µM). Then, aliquots of the cells were incubated in PBS/10 mM glucose in the presence of 1 µM MitoSOX for the determination of superoxide production, or 25 nM TMRM for the measurement of MMP. Fluorescence was detected using flow cytometric analysis. The left panel reports quantification of superoxide production (red bars). The right panel shows the MMP analysis in Jurkat cells where dark blue corresponds to the cell population with a low membrane potential, while light gray is related to the cell population with a high membrane potential.

Activation of the apoptotic pathway

The release of cytochrome *c* and the state of caspase 3 were examined in Jurkat cells exposed to the three TLMs or the organic tamoxifens for 18 h (Fig. 5).

The results clearly show that after incubation with the three TLMs, cytochrome *c* was released from the mitochondria to the cytosol, whereas it was still located in the mitochondria for the cells treated with organic tamoxifens. Moreover, pro-caspase 3 was only detected in the cells exposed to organic tamoxifens and not in the cells exposed to TLMs. Thus, only TLMs and not organic tamoxifens were able to trigger cell apoptosis by the mitochondria-mediated pathway.

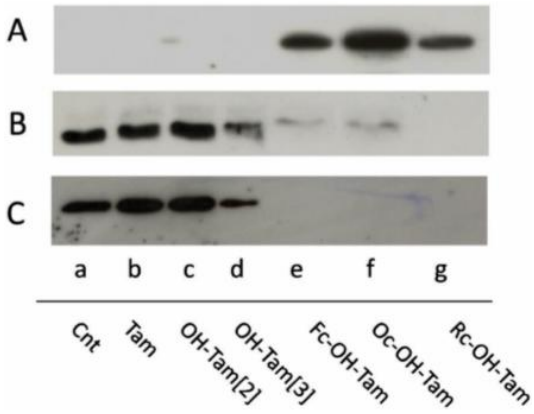

Fig. 5 Apoptosis pathway activation in Jurkat cells incubated with TLMs or tamoxifen derivatives. Jurkat cells (2 x 10^6) were treated for 18 h in the presence of 15 µM compounds. Cytochrome *c* localization was evaluated in the cytosol (A) and in the mitochondria (B); pro-caspase-3 detection is reported in (C). (a) **Cnt**; (b) **Tam**; (c) **OH-Tam[2]**; (d) **OH Tam[3]**; (e) **Fc-OH-Tam**; (f) **Oc-OH-Tam**; (g) **Rc-OH-Tam**.

Intracellular distribution of metals in Jurkat cells

As we found that metallocifens induced mitochondrial impairment we undertook, by ICP-OES, quantification of iron, ruthenium and osmium in the mitochondria and cytosol of cells exposed to **Fc-OH-Tam**, **Rc-OH-Tam** and **Oc-OH-Tam** (Table 3 and Fig. S6, ESI†). As iron is a metal present in cells, its quantification was also performed in untreated cells.

Table 3 ICP-OES quantification of iron, ruthenium and osmium in the cytosol and mitochondria of Jurkat cells incubated for 24 h with 30 µM **Fc-OH-Tam**, **Oc-OH-Tam** and **Rc-OH-Tam**, and of iron in untreated cells

Compound	Cytosol (nmol mg^{-1} protein)	Mitochondria (nmol mg^{-1} protein)
Fc-OH-Tam[a]	10 ± 5	153 ± 43
Oc-OH-Tam[b]	5.5 ± 4.9	108 ± 31
Rc-OH-Tam[c]	0.13[d]	75
Untreated cells (Fe)	1.5 ± 0.9	19 ± 11

[a] Mean of 3 experiments. [b] Mean of 2 experiments. [c] Single experiment. [d] Value in the range of the blanks.

The amounts of iron, osmium and ruthenium in the cytosol and in the mitochondria were in the same order of magnitude, indicating that the three TLMs were all able to

accumulate in cells, with a high concentration in the mitochondria. The amount of iron in the cytosol and mitochondria of cells incubated with 30 μM **Fc-OH-Tam** was significantly higher than the level of iron in the control cells, indicating that it mostly originated from **Fc-OH-Tam** and not from the endogenous iron pool.

The subcellular distribution of the metals gave an almost exclusive localization in the nuclear crude fractions (45–54%) and mitochondria (37–50%), and only a marginal localization in the cytosol (5–9%) (Table 4).

Table 4 Subcellular distribution (%) of Fe and Os in Jurkat cells incubated with 30 μM **Fc-OH-Tam** and **Oc-OH-Tam** for 24 h

Compound	Cytosolic fraction (%)	Mitochondrial fraction (%)	Crude nuclear fraction (%)
Fc-OH-Tam[a]	9 ± 2	37 ± 7	54 ± 9
Oc-OH-Tam[b]	5 ± 2	50 ± 7	45 ± 4

[a] Mean of 3 experiments. [b] Mean of 2 experiments.

Lipophilic cations are well known to preferentially localize in mitochondria.[34,35] At physiological pH, the dimethylamino group of TLMs is protonated, thus they can be considered as lipophilic cations. Consequently, they are expected to target mitochondria. Such behaviour is also encountered for other lipophilic metal-based drug candidates of gold(I),[36] osmium(II),[37] and rhenium(I).[38]

Discussion

In vitro inhibition of TrxR by TLMs occurred after their enzymatic oxidation by the HRP/H_2O_2 mixture, and the products of oxidation were in general more active on the cytosolic isoform (IC_{50} in the 0.06–1.2 μM range) than on the mitochondrial form (IC_{50} in the 3.9–10.9 μM range, Table 1). In contrast, oxidized organic tamoxifen derivatives were

much poorer inhibitors of TrxR, thus underlining the essential role played by the metallocenic entity in the oxidation profile and in the inactivation of TrxR. Independent spectroscopic studies showed that the species responsible for TrxR inhibition were their quinone methides for **Fc-OH-Tam** and **Rc-OH-Tam** and the quinone methide cation for **Oc-OH-Tam**, all of which displayed a highly electrophilic character. The inability of the HRP/H_2O_2 system to generate the QM of organic tamoxifens confirmed this assertion. Within the TLM series, the extent of inhibition depends on both the metallocene unit and the TrxR isoform. Oxidized **Fc-OH-Tam** was significantly less efficient on TrxR2 than **Rc-OH-Tam** and **Oc-OH-Tam** while the reverse was observed for TrxR1 for which oxidized **Fc-OH-Tam** was the most active (IC_{50} = 0.06 µM). This very low value is in the range of those measured for gold(I) complexes which are recognized as very potent inhibitors of TrxR.[14,39-41]

The mechanism of inhibition of TrxR1 by the oxidized TLMs was investigated by the BIAM assay. This assay demonstrated that only the 3 oxidized TLMs and not the organic tamoxifens interacted with the C-terminal redox active site of TrxR1. Oxidized **Fc-OH-Tam** and **Rc-OH-Tam** selectively interacted with the penultimate selenocysteine residue while oxidized **Oc-OH-Tam** was also able to interact with the cysteine residues. The fact that the product of oxidation of **Oc-OH-Tam** is a quinone methide carbocation[15] and not the neutral quinone methide may provide a rationale for this different reactivity.

Very different behaviour was observed in Jurkat cells, since the TLMs themselves were able to inhibit TrxR, indicating that their activation occurred *in cellulo* by endogenous oxidation systems. Moreover, all three TLMs were more efficient inhibitors of TrxR2 compared to TrxR1. This rather puzzling result is easily understandable when considering the subcellular distribution of the complexes, namely low concentrations in the cytosol and high concentrations in the mitochondria. Such an inversion of selectivity was previously noticed for cationic and lipophilic gold(I) complexes that displayed the same ability to preferentially accumulate in mitochondria.[42] The fact that inhibition of the mitochondrial thioredoxin system was coupled with alteration of the MMP, overproduction of ROS and translocation of cytochrome *c* may have to do with the recently reported deregulation of the redox state of cyclophilin D, a mitochondrial enzyme involved in the regulation of the mitochondrial permeability transition process.[43] In contrast, organic tamoxifens were far less potent TrxR inhibitors than metallocifens in cells. This finding is in line with the results on

purified TrxR and highlights again the essential input of the metallocenic units on the biological activity of TLMs.

Among the three TLMs, **Fc-OH-Tam** behaved differently from the two others regarding the redox state of Trx2, as cells incubated with **Fc-OH-Tam** contained 90% of the fully oxidized form of Trx2, but those incubated with **Rc-OH-Tam** and **Oc-OH-Tam** contained only 57%. **Fc-OH-Tam** also induced a higher level of mitochondrial superoxide and an early decrease in MMP.

These differences may be accountable to the much lower redox potential of ferrocene derivatives (+0.4 V for Fc,[7] *versus* +0.8 V for Rc,[44] and +0.6 V for Oc,[15] in their analogous metallociphenols). Indeed, according to Kovacic, only the metallocenes with a redox potential between +0.4 and -0.44 V display anticancer activity since this range of potential is favorable for *in vivo* electron transfer and redox cycling.[45] In our series, only **Fc-OH-Tam** fulfils this requirement.

Conclusion

We showed that TLMs became strong inhibitors of both isoforms of TrxR after their enzymatic oxidation with HRP/H_2O_2. All the oxidized TLMs were stronger inhibitors of the cytosolic isoform TrxR1 with **Fc-OH-Tam** showing a remarkably low IC_{50} value of 60 nM. In Jurkat cells, TLMs preferentially accumulated in the mitochondria as compared to the cytosol. Accordingly, they preferentially inhibited the mitochondrial isoform of TrxR and stimulated the oxidation of Trx2, leading to a cell redox imbalance.

The induced permeability of the mitochondrial membrane elicited the release of cytochrome *c* and activation of the caspase pathway, leading to cell apoptosis. This type of death found in Jurkat cells differs from that previously found in adherent tumour MDA-MB-231 cells, in which senescence was mainly observed. This study uncovers for the first time the powerful pro-apoptotic effects of TLMs, which appear to be responsible for their cytotoxicity in a lymphoblastoid cancer cell line and could be relevant for future clinical applications in the chemotherapy of resistant tumours.

Abbreviations

BIAM	Biotin iodoacetamide
DHR	Dihydrorhodamine 123
Fc-OH-Tam	1-[4-[3-(Dimethylamino)propyloxy]phenyl]-1-(4-hydroxyphenyl)-2-ferrocenyl-1-butene
HRP	Horseradish peroxidase
ICP-OES	Inductively coupled plasma optical emission spectroscopy
MMP	Mitochondrial membrane potential
Oc-OH-Tam	1-[4-[3-(Dimethylamino)propyloxy]phenyl]-1-(4-hydroxyphenyl)-2-osmocenyl-1-butene
Rc-OH-Tam	1-[4-[3-(Dimethylamino)propyloxy] phenyl]-1-(4-hydroxyphenyl)-2-ruthenocenyl-1-butene
Tam	Tamoxifen, 1-[4-[2-(Methylamino)ethoxy]phenyl]-1,2-diphenyl-1-but-1-en
OH-Tam[2]	4-Hydroxy-tamoxifen, (*E*/*Z*)-4-[1-[4-[2-(Methylamino) ethoxy]phenyl]-2-phenyl-1-buten-1-yl]-phenol
OH-Tam[3]	(*E*/*Z*)-4-[1-[4-[2-(Methylamino)propyl]phenyl]-2-phenyl-1-buten-1-yl]-phenol
RFU	Relative fluorescence unit
TLMs	Tamoxifen-like metallocifens
TMRM	Tetramethyl rhodamine methyl ester
TNBC	Triple negative breast cancer
TrxR	Thioredoxin reductase
TrxR1	Cytosolic thioredoxin reductase

TrxR2	Mitochondrial thioredoxin reductase
Trx	Thioredoxin

Acknowledgements

The authors acknowledge COST Actions CM1105 and CM1106 for financial support and for allowing fruitful collaboration, and Dr Benoit Caron and Dr Benoit Villemant in-charge of the ALIPP6 platform at the University Pierre et Marie Curie Paris for assistance in the ICP-OES experiments.

References

1 N. Harbeck and M. Gnant, Breast Cancer, *Lancet*, 2017, **389**, 1134–1150.

2 G. Jaouen, A. Vessieres and S. Top, Ferrocifen type anticancer drugs, *Chem. Soc. Rev.*, 2015, **44**, 8802–8817.

3 S. Top, A. Vessières, G. Leclercq, J. Quivy, J. Tang, J. Vaissermann, M. Huché and G. Jaouen, Synthesis, biochemical properties and molecular modelling studies of organometallic specific estrogen receptor modulators (SERMs), the ferrocifens and hydroxyferrocifens: evidence for an antiproliferative effect of hydroxyferrocifens on both hormone-dependent and hormone-independent breast cancer cell lines, *Chem. – Eur. J.*, 2003, **9**, 5223–5236.

4 A. L. Laine, E. Adriaenssens, A. Vessières, G. Jaouen, C. Corbet, E. Desruelles, P. Pigeon, R. A. Toillon and C. Passirani, The *in vivo* performance of ferrocenyl tamoxifen lipid nanocapsules in xenografted triple negative breast cancer, *Biomaterials*, 2013, **34**, 6949–6956.

5 Q. Michard, G. Jaouen, A. Vessières and B. A. Bernard, Evaluation of the cytotoxic properties of organometallic ferrocifens on melanocytes, primary and metastatic melanoma cells, *J. Inorg. Biochem.*, 2008, **102**, 1980–1985.

6 A. Vessières, C. Corbet, J. M. Heldt, N. Lories, N. Jouy, I. Laios, G. Leclercq, G. Jaouen and R. A. Toillon, A ferrocenyl derivative of hydroxytamoxifen elicits an estrogen receptor-independent mechanism of action in breast cancer cell lines, *J. Inorg. Biochem.*, 2010, **104**, 503–511.

7 E. A. Hillard, A. Vessières, L. Thouin, G. Jaouen and C. Amatore, Ferrocene-mediated proton-coupled electron transfer in a series of ferrocifen-type breast cancer drug candidates., *Angew. Chem., Int. Ed.*, 2006, **45**, 285–290.

8 A. Citta, A. Folda, A. Bindoli, P. Pascal Pigeon, S. Top, A. Vessières, M. Salmain, G. Jaouen and M. P. Rigobello, Evidence for targeting thioredoxin reductases with ferrocenyl quinone methides. A possible molecular basis for the anti-proliferative effect of hydroxyferrocifens on cancer cells, *J. Med. Chem.*, 2014, **57**, 8849–8859.

9 W. Q. Cai, L. W. Zhang, Y. L. Song, B. L. Wang, B. X. Zhang, X. M. Cui, G. M. Hu, Y. P. Liu, J. C. Wu and J. G. Fang, Small molecule inhibitors of mammalian thioredoxin reductase, *Free Radical Biol. Med.*, 2012, **52**, 257–265.

10 V. Gandin and A. P. Fernandes, Metal- and Semimetal- Containing Inhibitors of Thioredoxin Reductase as Anti-cancer Agents, *Molecules*, 2015, **20**, 12732–12756.

11 Y. Liu, Y. J. Li, S. H. Yu and G. S. Zhao, Recent Advances in the Development of Thioredoxin Reductase Inhibitors as Anticancer Agents, *Curr. Drug Targets*, 2012, **13**, 1432–1444.

12 F. Saccoccia, F. Angelucci, G. Boumis, D. Carotti, G. Desiato, A. E. Miele and A. Bellelli, Thioredoxin Reductase and its Inhibitors, *Curr. Protein Pept. Sci.*, 2014, **15**, 621–646.

13 A. Bindoli and M. P. Rigobello, Principles in Redox Signaling: From Chemistry to Functional Significance, *Antioxid. Redox Signaling*, 2013, **18**, 1557–1593.

14 A. Bindoli, M. P. Rigobello, G. Scutari, C. Gabbiani, A. Casini and L. Messori, Thioredoxin reductase: A target for gold compounds acting as potential anticancer drugs, *Coord. Chem. Rev.*, 2009, **253**, 1692–1707.

15 H. Z. S. Lee, O. Buriez, F. Chau, E. Labbé, R. Ganguly, C. Amatore, G. Jaouen, A.

Vessières, W. K. Leong and S. Top, Synthesis, characterization, and biological properties of osmium-based tamoxifen derivatives. Comparison with their homologues in the iron and ruthenium series, *Eur. J. Inorg. Chem.*, 2015, 4217–4225.

16 V. Scalcon, S. Top, H. Z. S. Lee, A. Citta, A. Folda, A. Bindoli, W. K. Leong, M. Salmain, A. Vessieres, G. Jaouen and M. P. Rigobello, Osmocenyl-tamoxifen derivatives target the thioredoxin system leading to a redox imbalance in Jurkat cells, *J. Inorg. Biochem.*, 2016, **160**, 296–304.

17 M. Luthman and A. Holmgren, Rat-liver thioredoxin and thioredoxin reductase – purification and characterization, *Biochemistry*, 1982, **21**, 6628–6633.

18 M. P. Rigobello and A. Bindoli, in *Methods in Enzymology: Thiol Redox Transitions in Cell Signaling, Pt B: Cellular Localization and Signaling*, ed. E. Cadenas and L. Packer, 2010, vol. 474, pp. 109–122.

19 O. H. Lowry, N. J. Rosebrough, A. L. Farr and R. J. Randall, Protein measurement with the folin phenol reagent, *J. Biol. Chem.*, 1951, **193**, 265–275.

20 J. G. Fang, J. Lu and A. Holmgren, Thioredoxin reductase is irreversibly modified by curcumin – A novel molecular mechanism for its anticancer activity, *J. Biol. Chem.*, 2005, **280**, 25284–25290.

21 S. Prast-Nielsen, M. Cebula, I. Pader and E. S. J. Arner, Noble metal targeting of thioredoxin reductase – covalent complexes with thioredoxin and thioredoxin-related protein of 14 kDa triggered by cisplatin, *Free Radical Biol. Med.*, 2010, **49**, 1765–1778.

22 D. A. Clayton and G. S. Shadel, Isolation of mitochondria from cells and tissues, *Cold Spring Harbor Protoc.*, 2014, DOI: 10.1101/pdbtop074542.

23 N. A. Bersani, J. R. Merwin, N. I. Lopez, G. D. Pearson and G. F. Merrill, Protein electrophoretic mobility shift assay to monitor redox state of thioredoxin in cells, *Methods Enzymol.*, 2002, **347**, 317–326.

24 J. Ungerstedt, Y. Du, H. Zhang, D. Nair and A. Holmgren, *In vivo* redox state of Human thioredoxin and redox shift by the histone deacetylase inhibitor suberoylanilide hydroxamic acid (SAHA), *Free Radical Biol. Med.*, 2012, **53**, 2002–2007.

25 P. Pigeon, S. Top, A. Vessières, M. Huché, E. A. Hillard, E. Salomon and G. Jaouen, Selective estrogen receptor modulators (SERMs) in the Ruthenocene series. Synthesis and biological behavior, *J. Med. Chem.*, 2005, **48**, 2814–2821.

26 S. Top, I. Efremenko, M. N. Rager, A. Vessieres, P. Yaswen, G. Jaouen and R. H. Fish, Derivatives Reacting with Cp*Rh Complexes that involve eta(1)-N, eta(2)-N,O, eta(1)-O, and eta(6) Bonding Modes, *Inorg. Chem.*, 2011, **50**, 271–284.

27 P. Messina, E. Labbé, O. Buriez, E. A. Hillard, A. Vessières, D. Hamels, S. Top, G. Jaouen, Y. M. Frapart, D. Mansuy and C. Amatore, Deciphering the activation sequence of ferrociphenol anticancer drug candidates, *Chem. – Eur. J.*, 2012, **18**, 6581–6587.

28 P. W. Fan, F. Zhang and J. L. Bolton, 4-hydroxylated metabolites of the antiestrogens tamoxifen and toremifene are metabolized to unusually stable quinone methides., *Chem. Res. Toxicol.*, 2000, **13**, 45–52.

29 A. M. Davies, M. E. Malone, E. A. Martin, R. M. Jones, R. Jukes, C. K. Lim, L. L. Smith and I. N. H. White, Peroxidase activation of 4-hydroxytamoxifen to free radicals detected by EPR spectroscopy, *Free Radical Biol. Med.*, 1997, **22**, 423–431.

30 M. I. Rybinskaya, A. Z. Kreindlin and S. S. Fadeeva, On the problem of stabilization of alpha-carbocationic centers in metallocene series – related interconversions of permethylated alpha-metallocenyl carbocations and metallocenium cation-radicals of the iron sub-group, *J. Organomet. Chem.*, 1988, **358**, 363–374.

31 M. I. Rybinskaya, A. Z. Kreindlin, Y. T. Struchkov and A. I. Yanovsky, On the problem of stabilization of alpha-metallocenyl carbocation – synthesis, properties and Crystal-structure of C5ME5OSC5ME4CH2 + BPH4-.CH2CL2, *J. Organomet. Chem.*, 1989, **359**, 233–243.

32 J. R. Kim, H. W. Yoon, K. S. Kwon, S. R. Lee and S. G. Rhee, Identification of proteins containing cysteine residues that are sensitive to oxidation by hydrogen peroxide at neutral pH, *Anal. Biochem.*, 2000, **283**, 214–221.

33 Y. T. Du, H. H. Zhang, X. Zhang, J. Lu and A. Holmgren, Thioredoxin 1 Is Inactivated

Due to Oxidation Induced by Peroxiredoxin under Oxidative Stress and Reactivated by the Glutaredoxin System, *J. Biol. Chem.*, 2013, **288**, 32241–32247.

34 A. Folda, A. Citta, V. Scalcon, T. Cali, F. Zonta, G. Scutari, A. Bindoli and M. P. Rigobello, Mitochondrial Thioredoxin System as a Modulator of Cyclophilin D Redox State, *Sci. Rep.*, 2016, **6**, 23071, DOI: 23010.21038/srep23071.

35 M. C. Frantz and P. Wipf, Mitochondria as a Target in Treatment, *Environ. Mol. Mutagen.*, 2010, **51**, 462–475.

36 L. Oehninger, R. Rubbiani and I. Ott, N-Heterocyclic carbene metal complexes in medicinal chemistry, *Dalton Trans.*, 2013, **42**, 3269–3284.

37 S. H. van Rijt, I. Romero-Canelon, Y. Fu, S. D. Shnyder and P. J. Sadler, Potent organometallic osmium compounds induce mitochondria-mediated apoptosis and S-phase cell cycle arrest in A549 non-small cell lung cancer cells, *Metallomics*, 2014, **6**, 1014–1022.

38 S. Imstepf, V. Pierroz, R. Rubbiani, M. Felber, T. Fox, G. Gasser and R. Alberto, Organometallic Rhenium Complexes Divert Doxorubicin to the Mitochondria, *Angew. Chem., Int. Ed.*, 2016, **55**, 2792–2795.

39 A. Citta, E. Schuh, F. Mohr, A. Folda, M. L. Massimino, A. Bindoli, A. Casini and M. P. Rigobello, Fluorescent silver(I) and gold(I)-N-heterocyclic carbene complexes with cytotoxic properties: mechanistic insights, *Metallomics*, 2013, **5**, 1006–1015.

40 O. Rackham, S. J. Nichols, P. J. Leedman, S. J. Berners-Price and A. Filipovska, A gold(I) phosphine complex selectively induces apoptosis in breast cancer cells: Implications for anticancer therapeutics targeted to mitochondria, *Biochem. Pharmacol.*, 2007, **74**, 992–1002.

41 E. Schuh, C. Pfluger, A. Citta, A. Folda, M. P. Rigobello, A. Bindoli, A. Casini and F. Mohr, Gold(I) Carbene Complexes Causing Thioredoxin 1 and Thioredoxin 2 Oxidation as Potential Anticancer Agents, *J. Med. Chem.*, 2012, **55**, 5518–5528.

42 O. Rackham, A. M. J. Shearwood, R. Thyer, E. McNamara, S. M. K. Davies, B. A. Callus, A. Miranda-Vizuete, S. J. Berners-Price, Q. Cheng, E. S. J. Arner and A.

Filipovska, Substrate and inhibitor specificities differ between human cytosolic and mitochondrial thioredoxin reductases: Implications for development of specific inhibitors, *Free Radical Biol. Med.*, **2011**, 50, 689–699.

43 A. P. Halestrap and A. P. Richardson, The mitochondrial permeability transition: A current perspective on its identity and role in ischaemia/reperfusion injury, *J. Mol. Cell. Cardiol.*, 2015, **78**, 129–141.

44 H. Z. S. Lee, O. Buriez, E. Labbé, S. Top, P. Pigeon, G. Jaouen, C. Amatore and W. K. Leong, Oxidative Sequence of a Ruthenocene-Based Anticancer Drug Candidate in a Basic Environment, *Organometallics*, 2014, **33**, 4940–4946.

45 P. Kovacic, Unifying mechanism for anticancer agents involving electron transfer and oxidative stress: Clinical implications, *Med. Hypotheses*, 2007, **69**, 510–516.

Electronic supplementary information

Table of contents

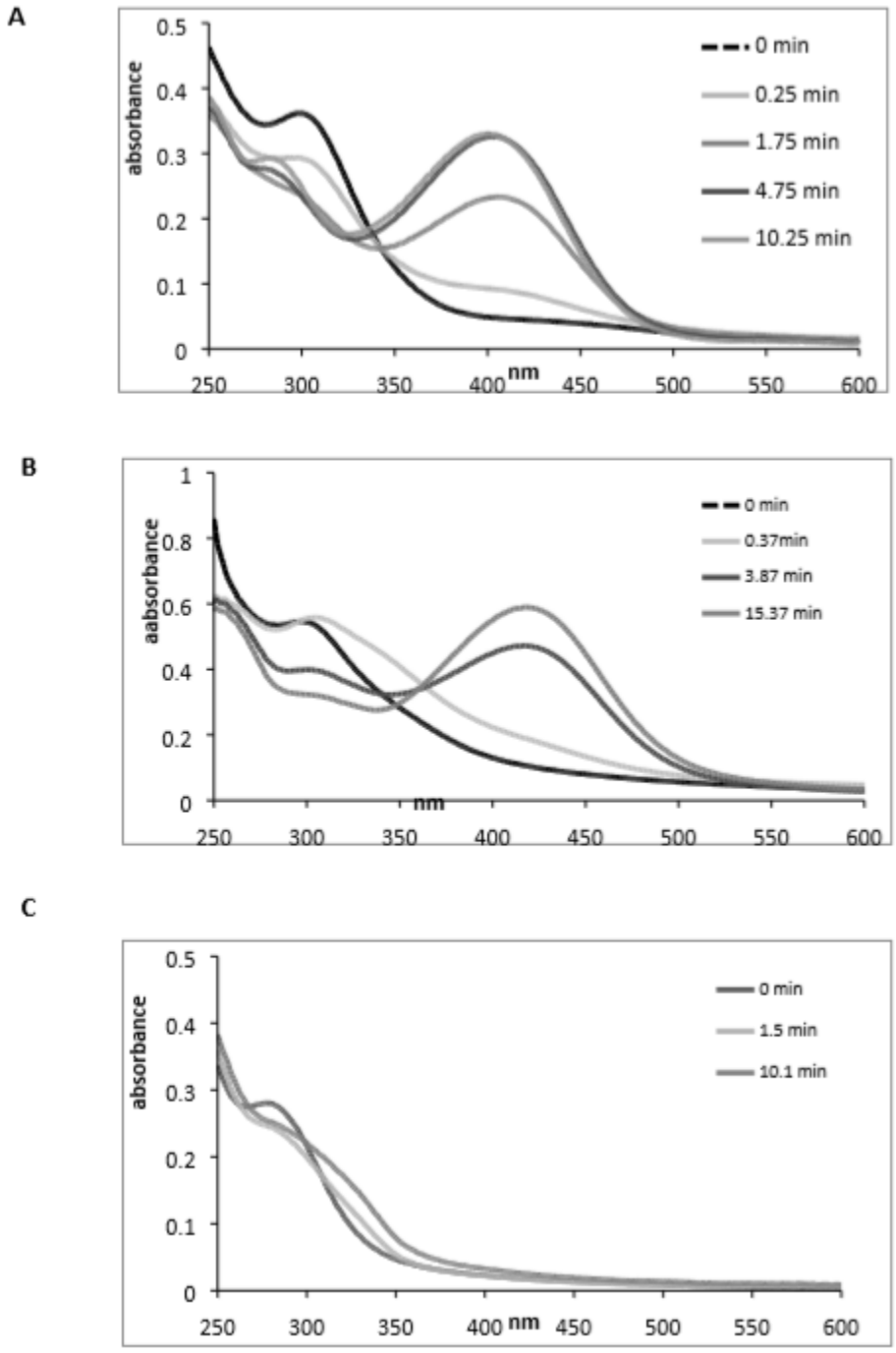

Fig.S1. UV-Vis spectral monitoring of enzymatic oxidation of Fc-OH-Tam (A), Rc-OH-Tam (B), or OHTam[3] (C). Each compound was mixed with HRP (44 nM) and H_2O_2 (200 µM) in 0.2 M Tris-HCl, 1 mM EDTA pH 8.1 and the UV-Vis spectra were recorded at the indicated times. Gradual appearance of a peak at 402 nm in the **Fc-OH-Tam** spectra (A) and a peak at 418 nm in the **Rc-OH-Tam** spectra **(B)** are assigned to the formation of the quinone methide derivatives. Disappearance of the peak at 279 nm for **OHTam[3] (C)** is assigned to its progressive oxidation without conversion to the quinone methide. (see Experimental Section for details)

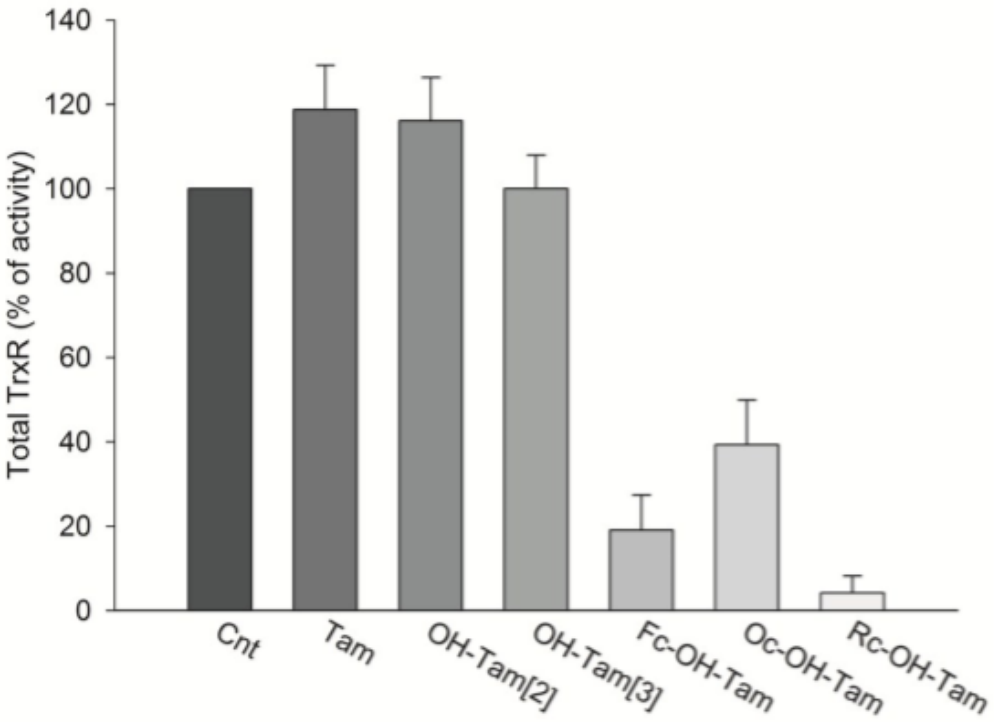

Fig. S2. Total TrxR activity in cell lysates. TrxR activity was determined after treatment of Jurkat cells (2 x 10^6) for 18 h with the indicated compounds (15 µM) following the procedure reported in the Experimental Section.

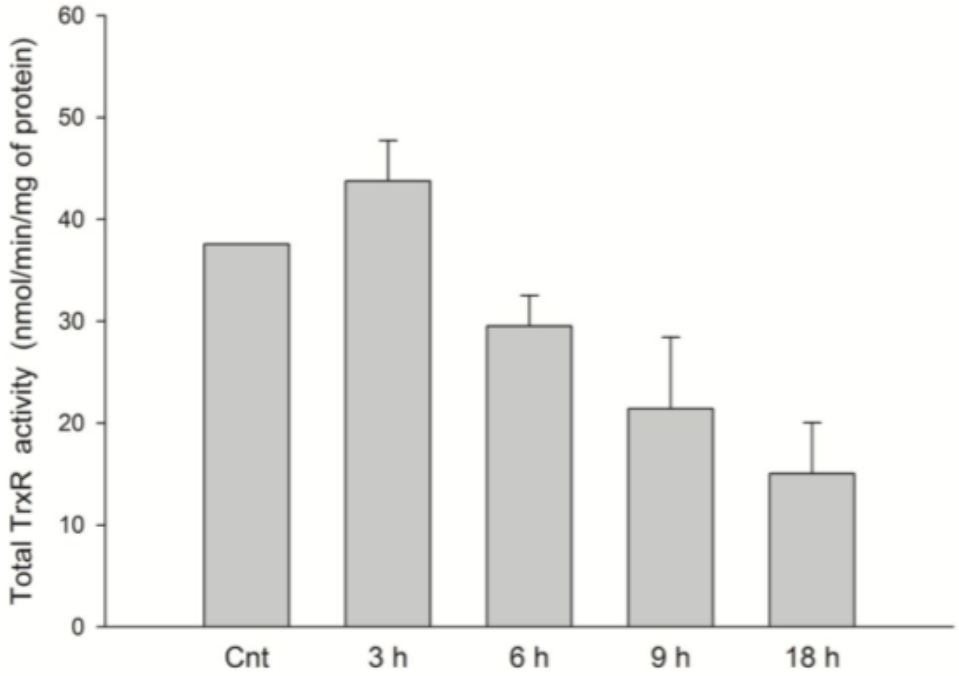

Fig. S3. Time scale of total TrxR activity in cell lysates after Fc-OH-Tam treatment. Jurkat cells (2 x 10^6) were treated for 3, 6, 9 or 18 h with 15 µM **Fc-OH-Tam**, then lysed and subjected to thioredoxin activity assay as described in Experimental Section.

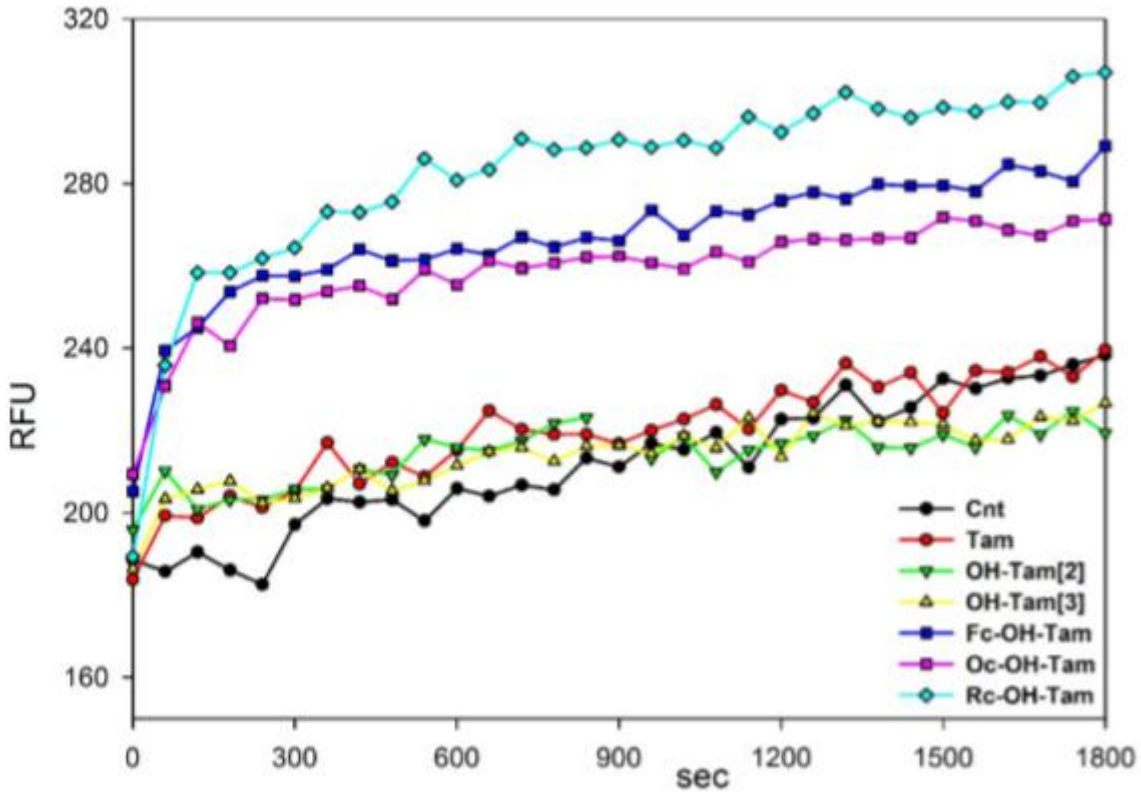

Fig. S4. Short-term ROS production of Jurkat cells after treatment with TLMs or organic tamoxifen derivatives. Jurkat cells (4 x 10^5/well) were incubated for 1 h with 15 µM DHR. Afterwards, the medium was removed and 10 µM compounds were added to the cells. Fluorescence increase was monitored on a plate reader as reported in Experimental Section.

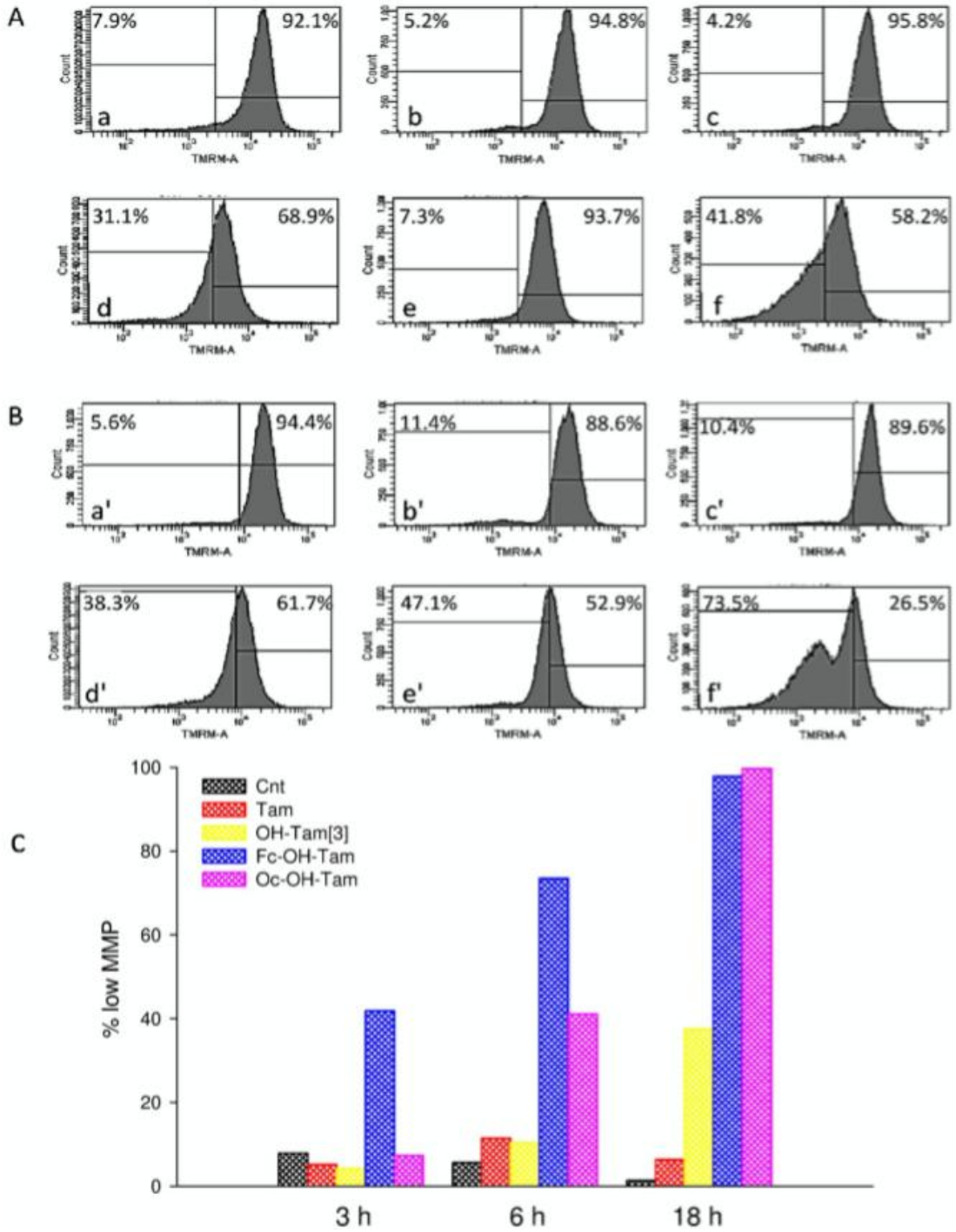

Fig. S5. Mitochondrial membrane potential (MMP) analysis of Jurkat cells after treatment with the various compounds at different incubation times. Cells (1 x 10^6) were treated for 3 h **(A)** or 6 h **(B)** with the indicated compounds (15 µM) and MMP was measured on 3 x 10^4 cells by flow cytometry analysis following TMRM fluorescence intensity (see Experimental Section). The two populations divided by the vertical gate correspond to cells with low MMP (left) and cells with high MMP (right). 1 µM carbonyl cyanide-m-chlorophenylhydrazone (CCCP), a classic uncoupling agent, was used as a positive control. a,a' **Cnt**; b,b' **Tam**; c,c' **OH-Tam[3]**; d,d' **CCCP**; e,e' **Oc-OH-Tam**; f,f' **Fc-OH-Tam. (C)** Percentage of Jurkat cells with low MMP in the range 3-18 h from the treatment with 15 µM compounds.

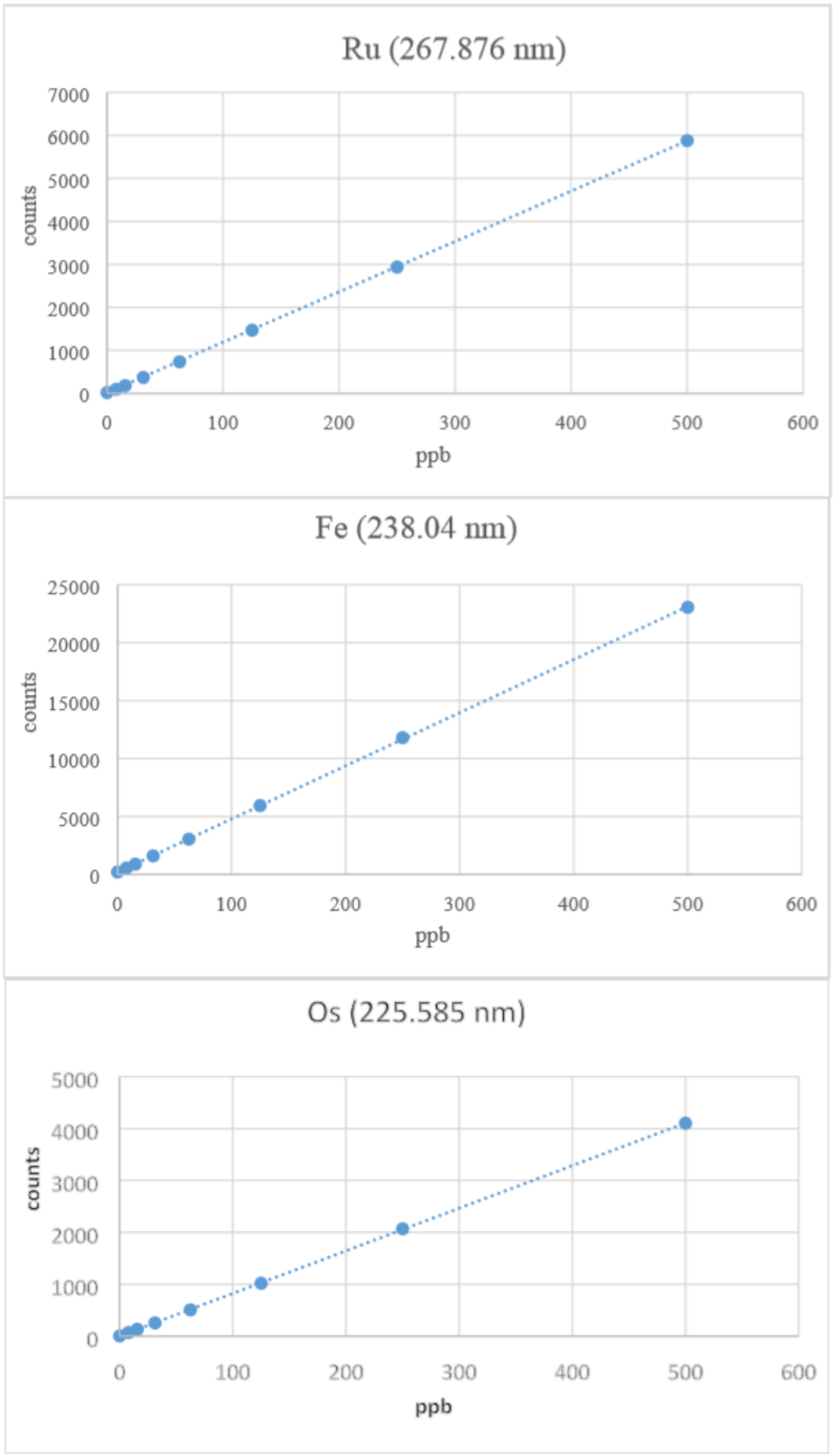

Fig. S6. Calibration curves for Ru, Fe, Os in the range (7.8 – 500 ppb) measured by ICP-OES